Table S1. Regional models driven by the ERA-Interim reanalysis from the European Centre for Medium-Range Weather Forecasts, for the 1989-2008 period.

RCM	Reference	acronym
CLMcom-CCLM4-8-17	Keuler et al. (2016)	CCLM
ETH-COSMO-crCLIM-v1-1	Pothapakula et al. (2020), Vautard et al. (2020)	ETH
CNRM-ALADIN53	Colin et al. (2010), Herrmann et al. (2011)	CNRM53
CNRM-ALADIN63	Daniel et al. (2019), Nabat et al. (2020)	CNRM63
DHMZ-RegCM4-2	Giorgi et al. (2012)	DHMZ
DMI-HIRHAM5	Christensen et al. (2007)	DMI
GERICS-REMO2015	Remedio et al. (2019)	GERICS
ICTP-RegCM4-6	Giorgi et al. (2012)	ICTP
IPSL-INERIS-WRF381P	Vautard et al. (2013)	IPSL
KNMI-RACMO22E	van Meijgaard et al. (2008)	KNMI
MPI-CSC-REMOO2009	Jacob et al. (2012)	MPI
SMHI-RCA4	Samuelsson et al. (2011)	SMHI
HadREM3-GA7-05	Tinker et al. (2015)	MOHC

Table S2. EURO-CORDEX Regional models driven by the CMIP5 GCMs. Also shown the approximate spatial resolution from each GCM taken from https://portal.enes.org/data/enes-model-data/cmip5/resolution. References: (A) Keuler et al. (2016) (B) Colin et al (2010), Herrmann et al (2011), (C) Daniel et al (2019), Nabat et al (2020), (D) Christensen et al. (2007), (E) Remedio et al. (2019), (F) Vautard et al. (2013), (G) van Meijgaard et al. (2008), (H) Samuelsson et al. (2011), (I) Tinker et al. (2015), (J) Giorgi et al. (2012), (K) Jacob et al. (2012).

CMIP5 GCM	Variant	Resolution	RCM	Reference	Acronym
CNRM-CERFACS-CNRM-CM5	r1i1p1	1.40° X 1.41°	CLMcom-CCLM4-8-17	A	CNRM-CCLM
			CNRM-ALADIN53	B	CNRM-CNRM53
			CNRM-ALADIN63	C	CNRM-CNRM63
			DMI-HIRHAM5	D	CNRM-DMI
			GERICS-REMO2015	E	CNRM-GERICS
			IPSL-WRF381P	F	CNRM-IPSL
			KNMI-RACMO22E	G	CNRM-KNMI
			SMHI-RCA4	H	CNRM-SMHI
ICHEC-EC-EARTH	r1i1p1	1.12° X 1.13°	DMI-HIRHAM5	D	ICHEC1-DMI
			KNMI-RACMO22E	G	ICHEC1-KNMI
			SMHI-RCA4	H	ICHEC1-SMHI
	r12i1p1		CLMcom-CCLM4-8-17	A	ICHEC2-CCLM
			ETH-COSMO-crCLIM-v1-1	A	ICHEC2-ETH
			DMI-HIRHAM5	D	ICHEC2-DMI
			IPSL-WRF381P	F	ICHEC2-IPSL
			KNMI-RACMO22E	G	ICHEC2-KNMI
			MOHC- HadREM3-GA7-05	I	ICHEC2-MOHC
			SMHI-RCA4	H	ICHEC2-SMHI
IPSL-CM5A-LR	r1i1p1	1.89° X 3.75°	GERICS-REMO2015	E	IPSL-GERICS
IPSL-CM5A-MR	r1i1p1	1.27° X 2.5°	IPSL-WRF381P	F	IPSL-IPSL
			KNMI-RACMO22E	G	IPSL-KNMI
			SMHI-RCA4	H	IPSL-SMHI
MPI-ESM-LR	r1i1p1	1.87° X 1.88°	CLMcom-CCLM4-8-17	A	MPI1-CCLM
			ETH-COSMO-crCLIM-v1-1	A	MPI1-ETH
			CNRM-ALADIN63	C	MPI1-CNRM63
			DMI-HIRHAM5	D	MPI1-DMI
			ICTP-RegCM4-6	J	MPI1-ICTP
			KNMI-RACMO22E	G	MPI1-KNMI
			MPI-REMO2009	K	MPI1-MPI
			SMHI-RCA4	H	MPI1-SMHI
	r2i1p1		ETH-COSMO-crCLIM-v1-1	A	MPI2-ETHZ
			MPI-REMO2009-MPI2-MPI	K	MPI2-MPI
			SMHI-RCA4	H	MPI2-SMHI
	r3i1p1		ETH-COSMO-crCLIM-v1-1	A	MPI3-ETH
			GERICS-REMO2015	E	MPI3-GERICS
			SMHI-RCA4	H	MPI3-SMHI
MOHC-HadGEM2-ES	r1i1p1	1.25° X 1.88°	CLMcom-CCLM4-8-17	A	MOHC-CCLM
			ETH-COSMO-crCLIM-v1-1	A	MOHC-ETH
			CNRM-ALADIN63	C	MOHC-CNRM
			DMI-HIRHAM5	D	MOHC-DMI
			ICTP-RegCM4-6	J	MOHC-ICTP
			IPSL-WRF381P	F	MOHC-IPSL
			KNMI-RACMO22E	G	MOHC-KNMI
			MOHC- HadREM3-GA7-05	I	MOHC-MOHC
			SMHI-RCA4	H	MOHC-SMHI
NCC-NorESM1-M	r1i1p1	1.89° X 2.5°	ETH-COSMO-crCLIM-v1-1	A	NCC-ETH
			DMI-HIRHAM5	D	NCC-DMI
			GERICS-REMO2015	E	NCC-GERICS
			IPSL-WRF381P	F	NCC-IPSL
			KNMI-RACMO22E	G	NCC-KNMI
			MOHC- HadREM3-GA7-05	I	NCC-MOHC
			SMHI-RCA4	H	NCC-SMHI
NOAA-GFDL-ESM2G	r1i1p1	2.02° X 2.00°	GERICS-REMO2015	E	NOAA-GERICS

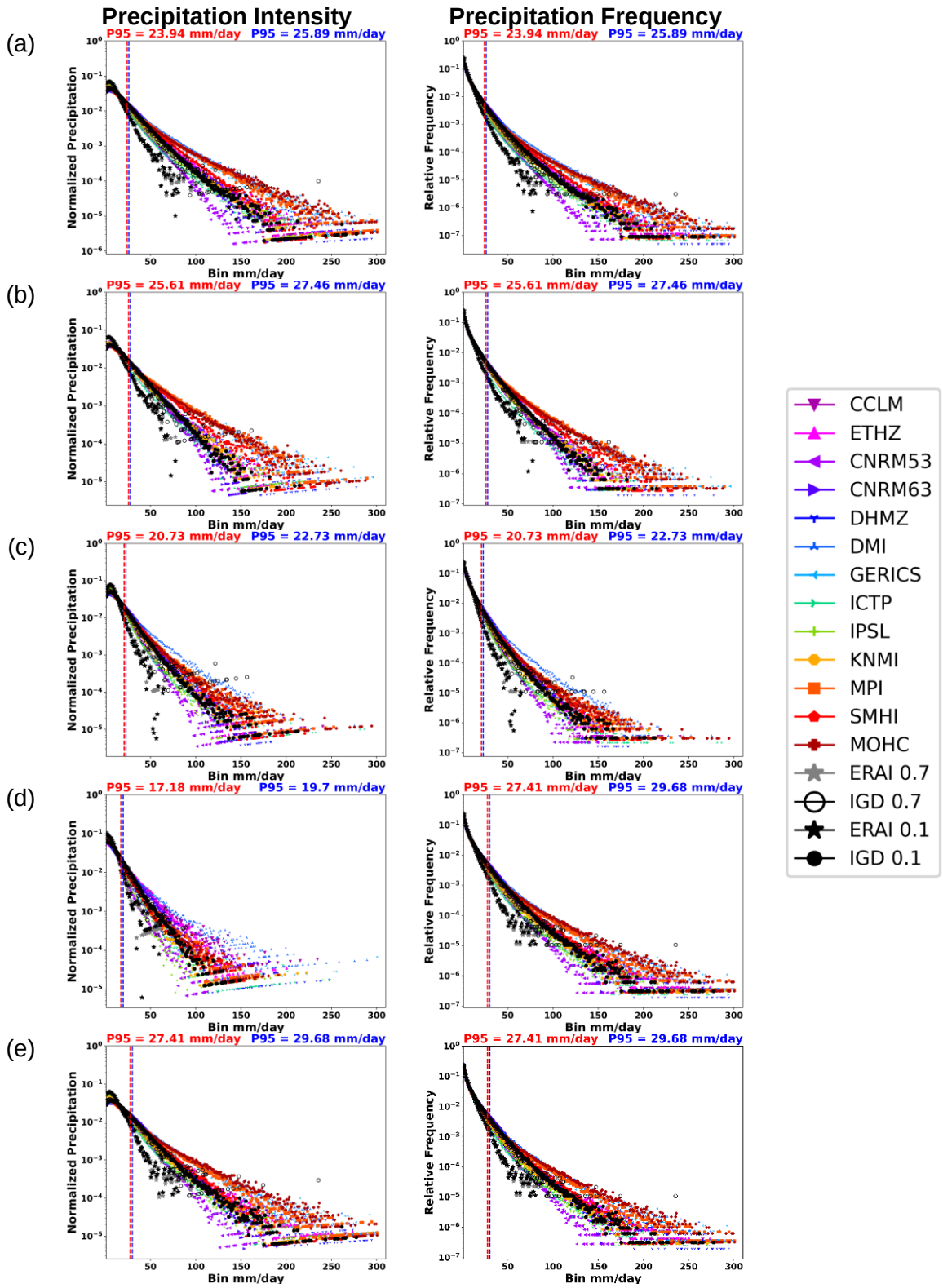

Figure S1. Daily precipitation Intensity (left) and frequency (right) distributions taken from the hindcast EURO-CORDEX RCMs and ERA-Interim reanalysis (1989-2008) for the Iberian Peninsula. Also shown the Iberian Gridded Dataset distribution for the same domain and period. All RCM data was previously interpolated into the IGD 0.1o regular resolution. As for Era-Interim, two PDFs are shown, one for the original resolution of the low-resolution and other interpolated into the IGD resolution. The dash point and the value written refers to the 95th percentile of the observations for NGD on the original resolution (blue) and interpolated into the ERA-Interim resolution (red). The time periods are (a) Year, (b) DJF, (c) MAM, (d) JJA and (e) SON.

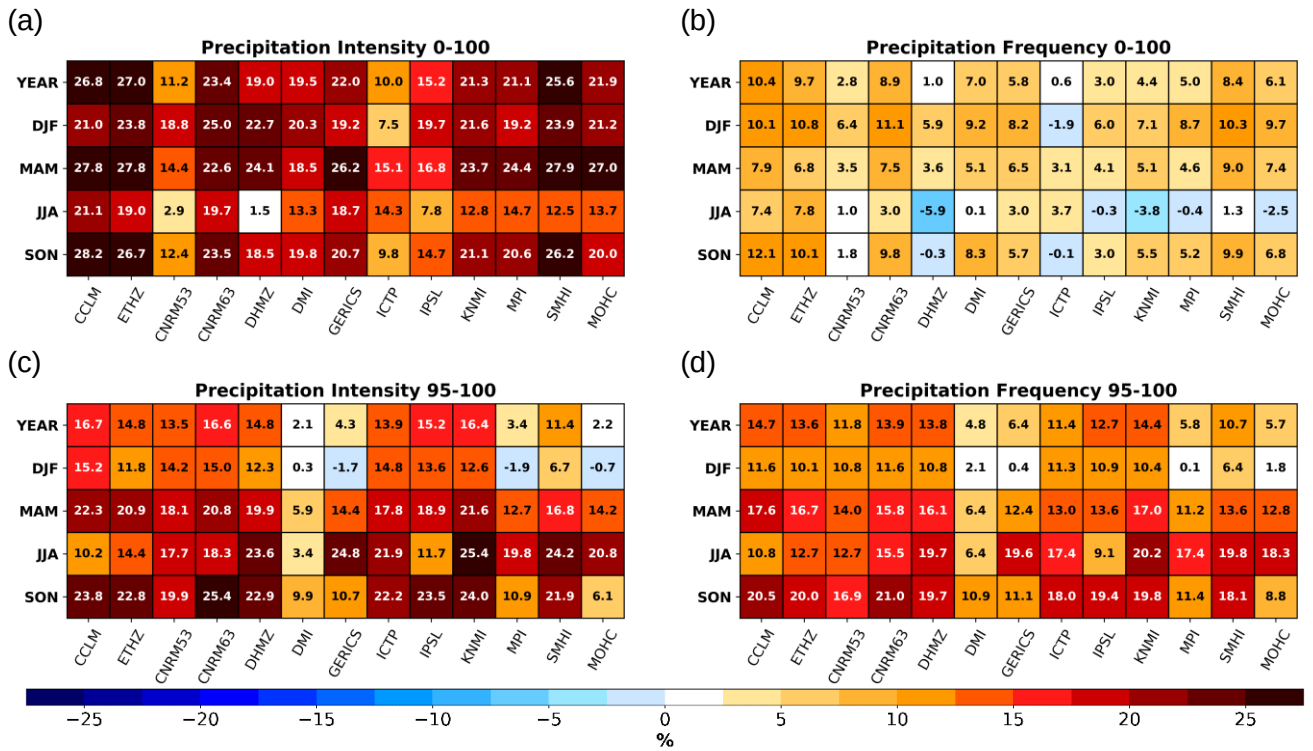

Figure S2. Yearly and seasonal distribution added values (DAV) of the Iberian Peninsula, between the RCMs and the ERA-Interim reanalysis for the 1989-2008 period, taken from the Hindcast EURO-CORDEX simulations, with the NGD regular dataset as reference for (a) daily precipitation intensity, considering the whole PDF shown in the left panels of Figure S1, (b) daily precipitation frequency considering the whole PDF shown in the right panels of Figure S1, (c) daily precipitation intensity extremes, only considering the values above the observational 95th percentile shown in Figure S1 left side and (d) daily precipitation frequency extremes, only considering the values above the observational 95th percentile shown in the right side of Figure S1. All model data were previously interpolated to 0.1^{o} regular resolution from the observations.

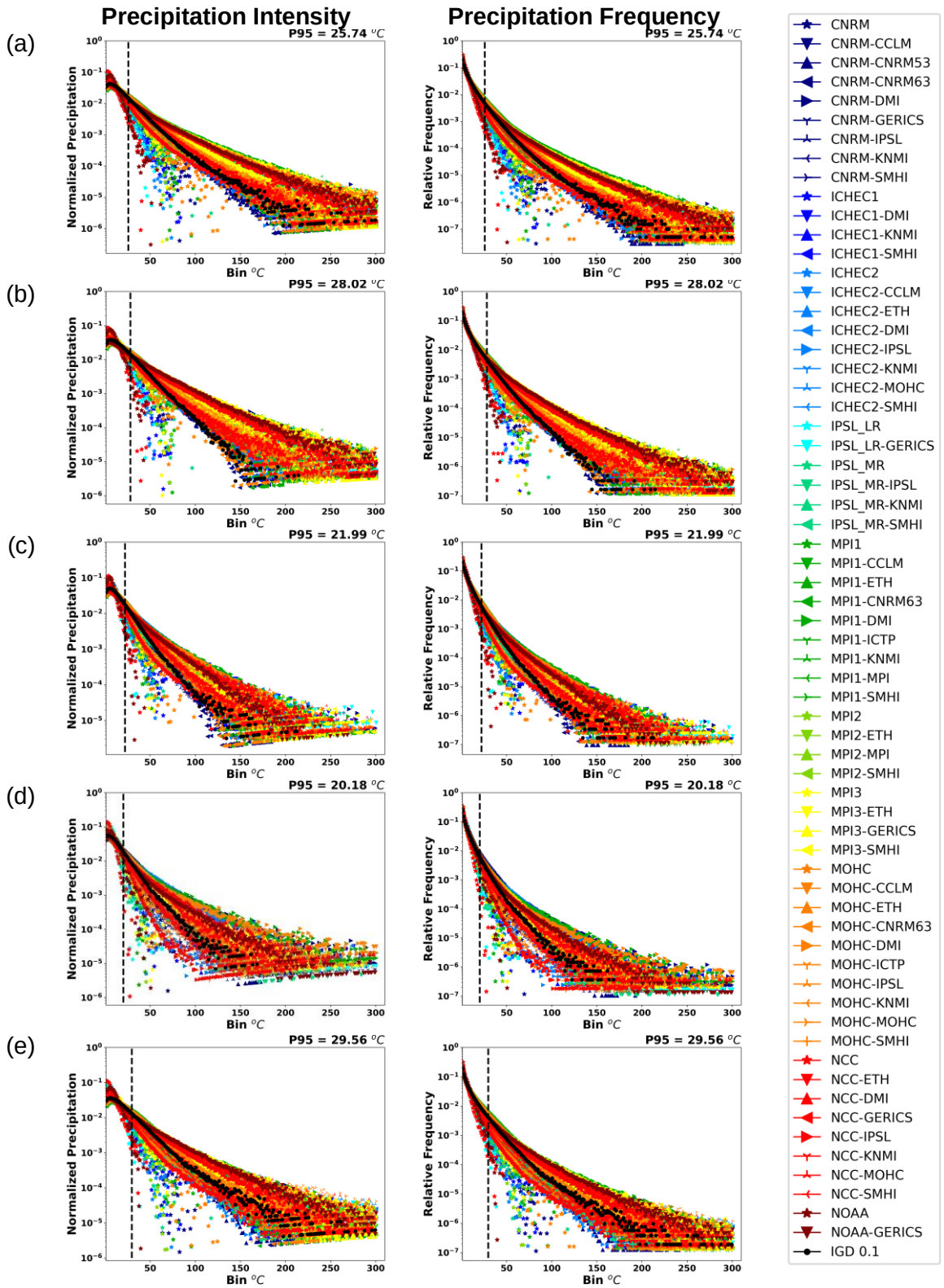

Figure S3. Daily precipitation Intensity (left) and frequency (right) for the historical driving CMIP5 GCMs and EURO-CORDEX RCMs for the Iberian Peninsula, considering the 1971-2005 period, where all results were previously interpolated into the observational grid. The dash point and the value written refers to the 95th percentile of the observations. (a) Year, (b) DJF, (c) MAM, (d) JJA and (e) SON.

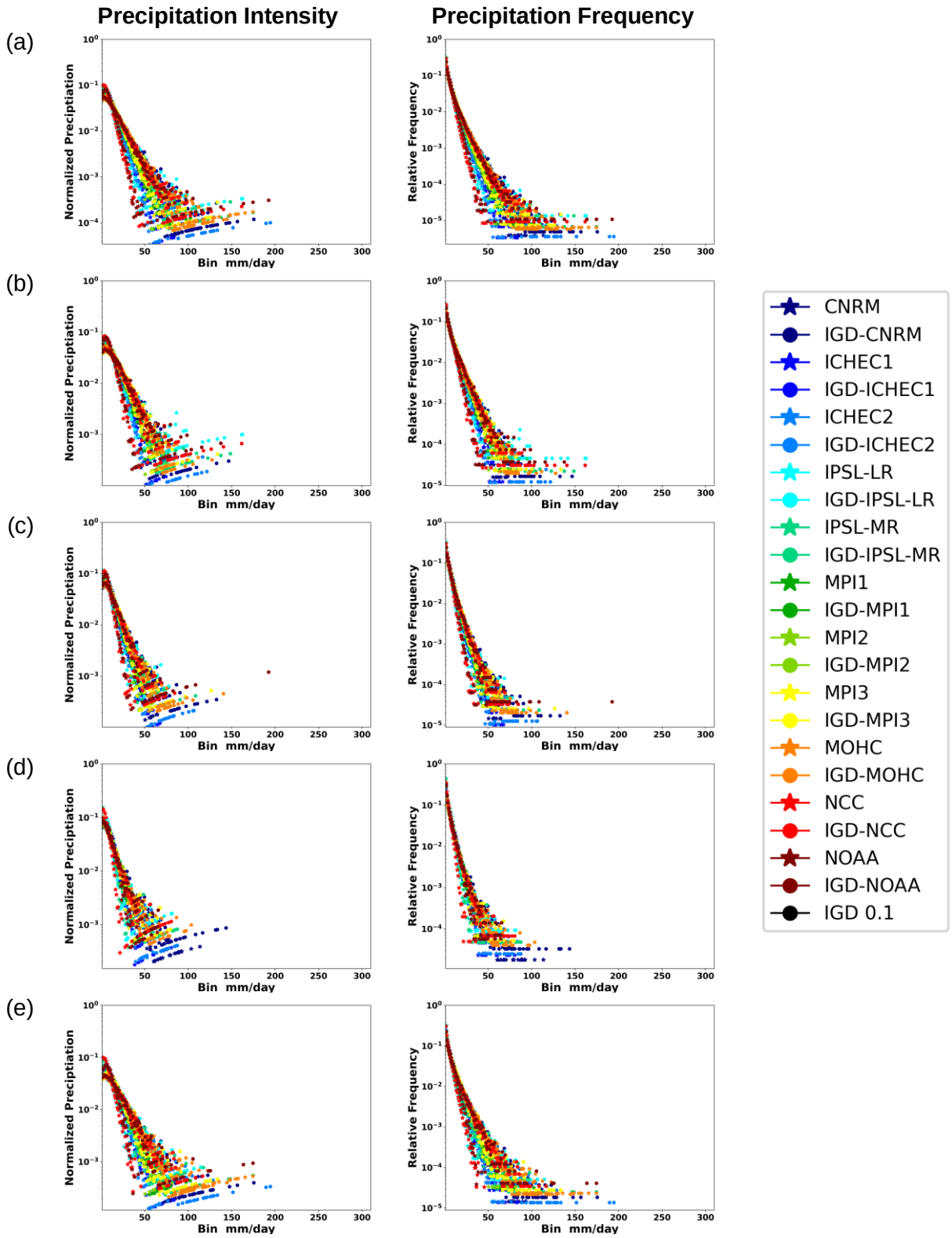

Figure S4. Daily precipitation Intensity (left) and frequency (right) for the historical driving CMIP5 GCMs and NGD observations interpolated into each GCM resolution for the Iberian Peninsula, considering the 1971-2005 period. Also shown the PDF from the NGD observations at the original resolution. (a) Year, (b) DJF, (c) MAM, (d) JJA and (e) SON.

(a)

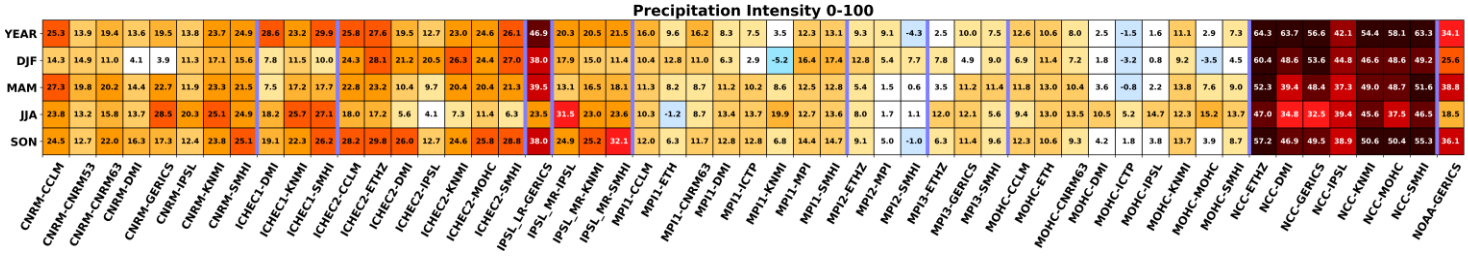

(b)

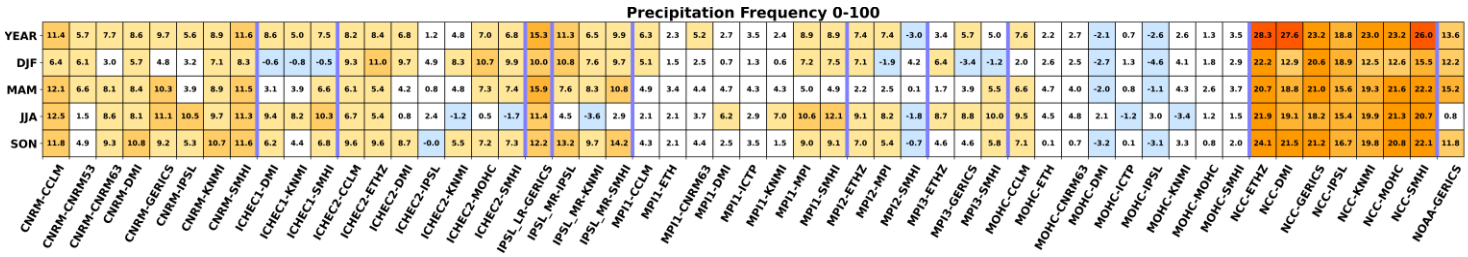

(c)

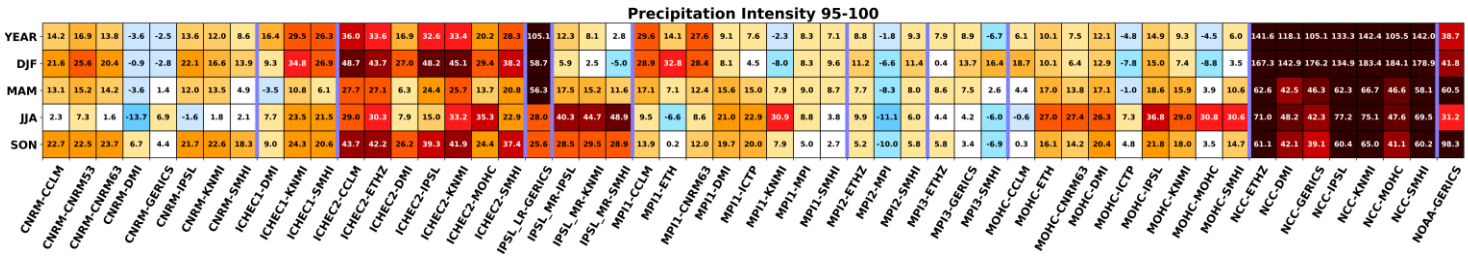

(d)

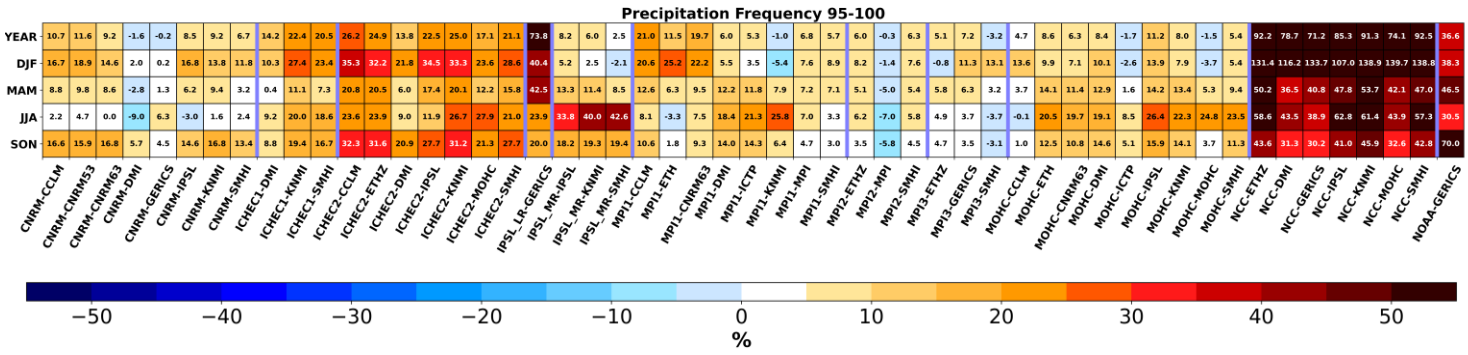

Figure S5. Yearly and seasonal distribution added values (DAV) of the Iberian Peninsula, between the RCMs and the CMIP5 GCMs for the 1989-2008 period, taken from the Historical EURO-CORDEX simulations, with the NGD regular dataset as reference for (a) daily precipitation intensity, considering the whole PDF shown in the left panels of Figure S3, (b) daily precipitation frequency considering the whole PDF shown in the right panels of Figure S3, (c) daily precipitation intensity extremes, only considering the values above the observational 95th percentile shown in Figure S3 left side and (d) daily precipitation frequency extremes, only considering the values above the observational 95th percentile shown in the right side of Figure S1. All model data were previously interpolated to 0.1º regular resolution from the observations.